Method to Extract Frequency Dependent Material Attenuation for Improved Transducer Models

Martin Angerer, Michael Zapf, Julia Koppenhöfer, and Nicole V. Ruiter

Institute for Data Processing and Electronics, *Karlsruhe Institute of Technology (KIT)*
Eggenstein-Leopoldshafen, Germany. Email: Martin.Angerer@kit.edu

***Abstract*—The time response of the ultrasound transducers used in our 3D ultrasound tomography device shows a slight reverberation. This may causes artifacts in the reconstructed images. Loss properties of materials used in the array fabrication have a big impact on their complex vibration behavior. Unfortunately, material parameters for accurate modeling are often not available in literature. Here, we present a method to derive loss properties of polymers and composites and how to include them in a finite element analysis (FEA). The method has three steps: First, an experiment to measure the frequency and thickness dependent sound attenuation. Second, a brute-force fit to a frequency-power law expression to obtain an analytic formulation. Third, a conversion of the sound attenuation to an equivalent structural loss factor. The last step is necessary as acoustic attenuation can not directly be implemented in structural mechanics FEA. We applied the method to derive loss properties of the filler and backing material which we use for our ultrasound transducer arrays. When including the loss factor in the simulation a reverberation is predicted, which matches the measurement well. Hence, considering loss properties allows more accurate modeling of complex vibration behavior. This aids in optimizing our ultrasound transducer array design towards better 3D ultrasound imaging.**

***Index Terms*—vibration damping; acoustic attenuation; structural loss factor; loss factor conversion; ultrasound transducers**

I. Introduction

Ultrasound Computer Tomography (USCT) is an emerging imaging approach for early breast cancer screening [1]. In comparison to mammography and magnetic resonance imaging, ultrasound is essentially harmless, cost-effective and does not require the use of potentially harmful contrast agents [2], [3]. At the Karlsruhe Institute of Technology we are working on a full 3D USCT system which allows simultaneous reflection and transmission imaging [4].

The requirements emanating from the applied image reconstruction algorithms resulted in a special transducer array design, schematically shown in Fig. 1 [5], [6]. There, 18 piezoceramic fibers with a diameter of 0.46 mm and a thickness of 0.6 mm are embedded in a filler material. The fibers are pseudo-randomly distributed on a 35.5 mm diameter disk [7]. This disk is then sandwiched between a PCB and a matching layer to form functional ultrasound transducer arrays.

The pulse response in water of a representative transducer is shown in Fig. 2. There, reverberation after the main pulse can be observed, which is also reflected in ripples in the corresponding frequency spectrum. This reverberation may cause artifacts in the reconstructed images and is therefore an undesirable effect [8].

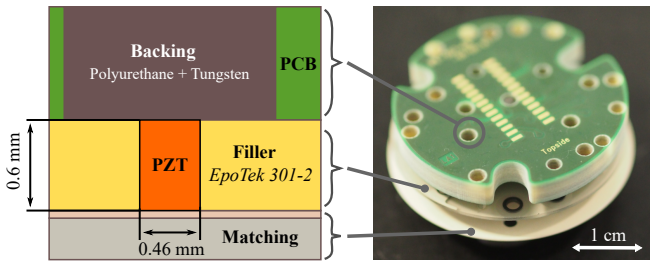

Fig. 1. Assembly of ultrasound transducer arrays used for our USCT system. A piezoceramic fiber is embedded in a filler material, and connected on front and back side to achieve the desired performance.

Internal transducer reverberation often arises from sound reflections on edges and surfaces within the transducer [9]. Another factor is the vibration behavior of the piezoceramic material, which ideally exhibits high frequency separation between distinct resonance modes. For our transducers, the low thickness-to-diameter ratio of $0.6/0.46$ leads to a small separation between the thickness and lateral mode and hence, to complex oscillation behavior [10].

To understand the origin of the reverberation, an accurate transducer model is needed. There, a key challenge is to obtain all necessary material parameters. Frequency-dependent loss properties are often not given in literature, but play an important role in modeling the vibration behavior correctly. Fig. 3

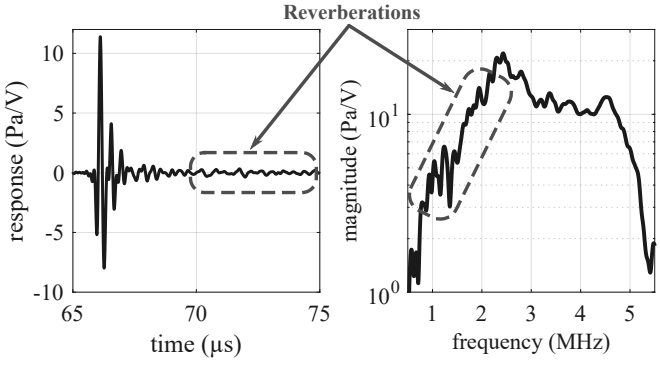

Fig. 2. Measured time response and the corresponding frequency spectrum of one representative transducer. The reverberations are reflected as additional signals after the main pulse and ripples in the spectrum.

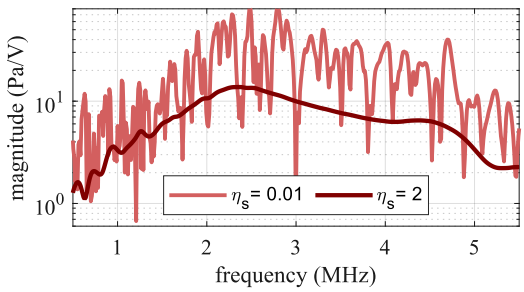

Fig. 3. Frequency response from FEA of one USCT transducer with varying loss factors η_s for the backing and filler material.

shows the effect of low and high damping on the simulated frequency response of our transducers. Low damping results in a non-uniform response with high ripples throughout the spectrum. High damping shows too uniform behavior when comparing it with the measurement in Fig. 2. The true damping values are somewhere in between these two parameters. In this paper we present a method to derive this frequency-dependent material damping from measurement and use it in FEA.

II. Materials and Methods

In acoustics, losses can be described mathematically according to Eq. 1 [11]. There, p_0 is the initial sound pressure, ω the angular frequency, v the speed of sound and α the medium specific sound attenuation coefficient.

$$p(x) = p_0 \cdot e^{-\alpha x} \cdot cos(\omega/v \cdot x) \tag{1}$$

To obtain loss properties of the backing and filler material, we applied the following method. First, an experiment was conducted to measure α with high precision and accuracy. Next the data was fitted to an analytic expression. Then an approach how to convert α to an equivalent structural loss factor η_s is presented, which is a suitable method for many FEA tools to account for damping.

A. Sound attenuation measurement

To obtain α for the filler and the backing material, we conducted an ultrasound transmission experiment. Four samples from each material with a diameter of 30 mm and varying thicknesses were produced. These samples were placed in a water tank in between two transducers and exposed to ultrasonic pulses (see Fig. 4). A signal processing chain with broadband chirps, coded excitation, matched filtering and averaging was developed to achieve sufficient signal strength for samples which exhibit high damping [12].

The attenuation was obtained for each sample by comparing the amplitudes of the transmission signal with an empty measurement. Surface reflections were compensated by normalizing the results with the transmission coefficient T, calculated from the acoustic impedances Z of the materials according to Eq. 2.

$$T = 4 \cdot Z_{water} Z_{mat} / (Z_{water} + Z_{mat})^2 \tag{2}$$

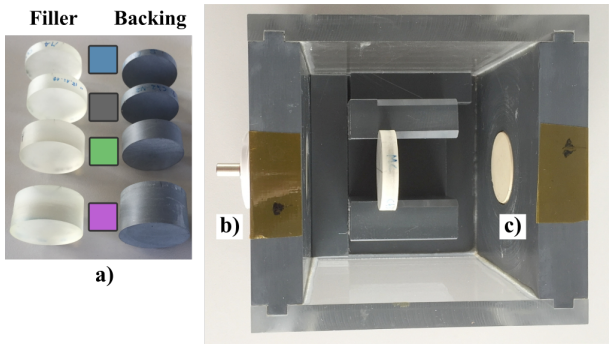

Fig. 4. Ultrasound transmission setup to measure acoustic material properties. Four samples (a) from the filler and backing material were exposed to ultrasound pulses (color matches results in Fig. 5). The signals are generated by the emitting transducer (b), pass through the water filled container and the material sample and are recorded by the receiver (c).

Fig. 5a and 5b show the measured α of the filler and backing material for each of the four material samples. A relationship between the attenuation and two properties can be clearly stated: The thicker the sample, the higher the attenuation. In addition, a significant nonlinear rise with frequency is present.

Even though we put much effort in obtaining high signal-to-noise, the range of the measured attenuation exhibits some limitation. Attenuations above 30 dB show high deviations from the expected trend. In addition, the frequency range is limited by the used ultrasound transducers. For the subsequent model fit we therefore excluded all data indicated with the grey areas in Fig. 5a and 5b.

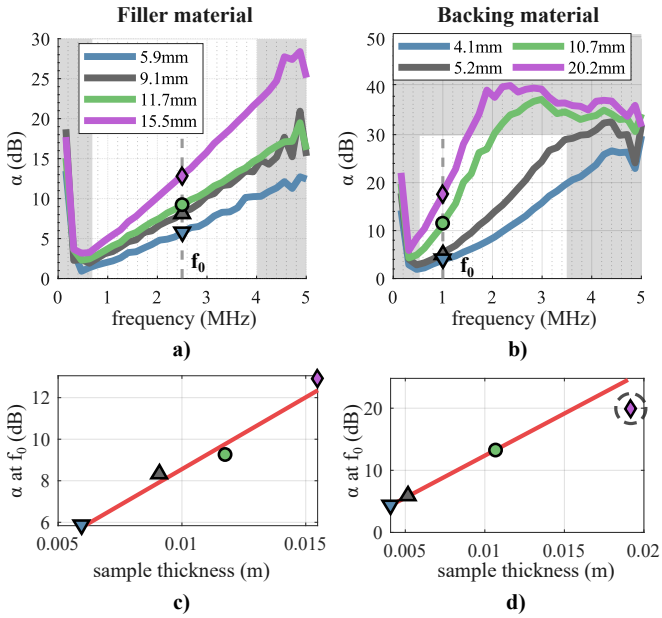

Fig. 5. Measured frequency and thickness dependent sound attenuation α of the filler material (a) and the backing material (b). At f_0, linear regression was calculated to obtain the relationship between attenuation α and the material thickness d. The grey areas in (a) and (b) indicate the frequency and attenuation ranges where data was excluded from the subsequent model fit.

B. Model fit

To model the attenuation as a function of the thickness and frequency, we used the frequency-power law according to Eq. 3 [13]. There, β is a positive number describing the loss behavior, a_0 is the attenuation at the frequency f_0 and the factor 8.7 is the conversion from Neper to dB.

$$\alpha(f,d) = 1/8.7 \cdot a_0 (f/f_0)^{\beta} \;\text{ with }\; a_0 = a_1 d + a_2 \tag{3}$$

The relation between a_0 (in dB) and the material thickness d is assumed to be linear. The coefficients a_1 and a_2 were therefore derived from linear regression as shown in Fig. 5c for the filler, and Fig. 5d for the backing. The regression was calculated at distinct frequencies f_0 for each material to obtain valid data. However, the thickest backing sample was excluded as it deviates significantly from linear regression.

To obtain the best fit parameters, a brute-force optimization by varying β was conducted. Typical values for β of polymers are in the range of 1 to 1.4 [14]. Therefore, this range was extended by 0.2 towards lower and higher values. The modeling results were evaluated with respect to the measurement using least-square minimization (see [10] for more details). The resulting best-fit parameters are listed in Tab. I.

The calculated attenuation using the best-fit parameters compared with the four measured material samples is shown in Fig. 6a and 6b for the filler and the backing material respectively. The attenuation behavior can be predicted with an overall fit accuracy of 55% for the filler, and 53% for the backing. These relatively low fits result from a single sample of each material and are likely caused by slightly varying measurement conditions and limits of the experimental setup.

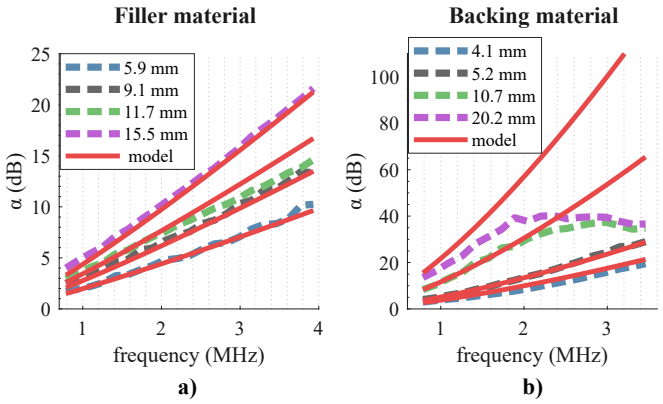

Fig. 6. Model-to-measurement comparison when using the best-fit parameters of β for the filler (a) and the backing material (b).

TABLE I
BEST-FIT MODEL PARAMETERS FOR THE ANALYTIC EXPRESSION OF α.

Parameter	Unit	Filler	Backing
f_0	MHz	2.5	1
β	-	1.16	1.39
a_1	dB/m	727	1035
a_2	dB	1.44	0.73

C. Attenuation model conversion

The utilized FEA tool (Comsol Multiphysics) does not support the direct use of acoustic attenuation in solids. An alternative way to account for damping is a hysteretic stiffness model. There, the structural loss factor η_s is added to the materials spring constant as a complex factor [15]. To use the derived expression in a FEA, we converted α to an equivalent structural loss factor η_s, as explained below.

Linear viscous damping is described by Eq. 4, where ξ is the viscous damping ratio, ω_0 the natural frequency and u_0 the initial amplitude.

$$u(t) = u_0 \cdot e^{-\xi\omega_0 \cdot t} \cdot cos(\omega t) \tag{4}$$

When invoking $\xi \approx \eta_s/2$ and converting from the time to the spatial domain using $t = x/v$, Eq. 4 can be rewritten according to Eq. 5.

$$u(x) = u_0 \cdot e^{-\frac{\eta_s \omega_0}{2v} \cdot x} \cdot cos(\omega/v \cdot x) \tag{5}$$

The relation in Eq. 6 between α and η_s can be derived when comparing Eq. 1 with Eq. 5, similarly stated in [16].

$$\eta_s(f,d) = 2v/\omega_0 \cdot \alpha(f,d) \;\text{ with }\; \omega_0 = \sqrt{k/m} \tag{6}$$

A valid assumption for polymers is that they exhibit viscoelastic damping properties [17]. With that assumption, the spring constant k can be approximated by $k = E \cdot s/L$ [15]. There, E is the materials modulus, s the cross section and L the effective length of the damping material. This finally leads to the expression in Eq. 7, where ρ is the density of the material.

$$\eta_s(f,d) = 2vL \cdot \alpha(f,d) \cdot \sqrt{\rho/E} \tag{7}$$

III. RESULTS

When applying the presented method, we obtain structural loss factors for the filler and backing material as shown in Fig. 7a. The backing exhibits very high losses with rising frequencies. At approx. 1 MHz it exceeds η_s values of 2, which represents the threshold for overdamping. The filler material has a much lower attenuation in the given frequency range. It does not reach the threshold, which from theory causes additional oscillation after an impulse response. To illustrate the different behavior Fig. 7b shows an example of a 2.5 MHz ringdown for both materials.

The results of the FEA using the derived loss factors compared to the representative measurement is shown in Fig. 8. Some reverberations are predicted in the pulse response, as the magnified view shows. These reverberations cause prominent ripples in the spectrum below 3 MHz, which matches well with the measurement. However, earlier reverberations which occur at approx. 68 µs are not covered.

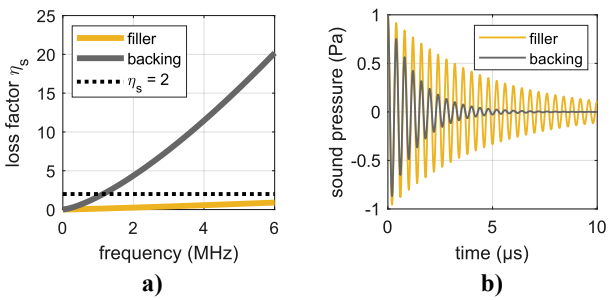

Fig. 7. (a) Structural loss factors $\eta_s(f)$ of the two materials derived with the presented method. (b) Example of a ringdown of $f = 2.5$ MHz for both materials in the time domain.

IV. Discussion and Conclusion

Comparing the measured USCT transducer responses with the FEA results shows that complex vibration behavior of transducers can be modeled by accurately considering material loss properties. Though not all measured reverberations are predictable, it still allows the identification and optimization of some unwanted effects. To more accurately cover the ringdown and earlier reverberation, the acoustic properties of the matching material have to be investigated in more detail.

After first analysis, the reverberations can be mapped to the multimodal vibration behavior of our transducers. The lateral damping (filler material) shows to be insufficient, especially for frequencies below 3 MHz, to fully counteract this effect. Different polymers or polymer-composites can now be evaluated systematically to further increase the damping.

The frequency- and thickness-dependent sound attenuation α can be determined with high precision and accuracy with the measurement setup used. In principle, only two samples per material would be necessary, but more samples are recommended to make the derivation more robust.

Frequency-power law is suitable to model α of not only polymers but also composite materials, which are widely used for acoustic backing. Converting α to an equivalent loss factor η_s enables the use of material loss properties in different modeling environments. This allows for a more comprehensive transducer design approach.

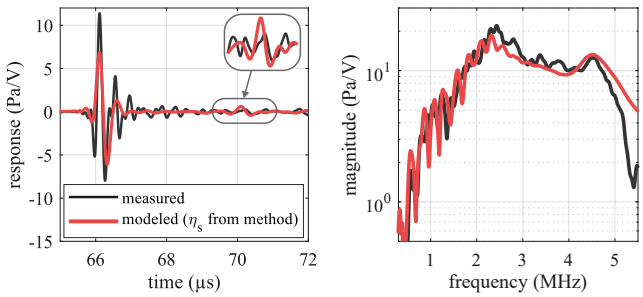

Fig. 8. Model-to-measurement comparison of a single representative ultrasound transducer in the time and frequency domain.

To derive η_s from the acoustic attenuation, the effective geometry of the damping material has to be assumed. Deriving η_s directly from a material analysis with dynamic mechanic excitation would therefore be more straightforward. However, with the presented experiment also the material's speed of sound and acoustic attenuation can be obtained. Therefore, the method gives a tool to derive multiple important material properties simultaneously.

In summary, the presented method allows to derive and model loss behavior of polymers and composites. Considering this loss behavior in FEA allows more accurate modeling of complex vibration behavior. In case of our USCT transducers, it enabled the simulation of some of the reverberation. This aids in optimizing our ultrasound transducer array design towards better 3D ultrasound imaging.

References

[1] N. Duric, P. Littrup, C. Li, O. Roy, S. Schmidt, R. Janer, X. Cheng, J. Goll, O. Rama, L. Bey-Knight, and W. Greenway, "Breast ultrasound tomography: Bridging the gap to clinical practice," *Progress in Biomedical Optics and Imaging - Proceedings of SPIE*, vol. 8320, p. 23, 2012.

[2] L. Lin, P. Hu, J. Shi, C. M. Appleton, K. Maslov, L. Li, R. Zhang, and L. V. Wang, "Single-breath-hold photoacoustic computed tomography of the breast," *Nature Communications*, vol. 9, no. 1, p. 2352, 2018.

[3] K. J. Opieliński, P. Pruchnicki, T. Gudra, P. Podgórski, J. Kurcz, T. Krasnicki, M. Sasiadek, and J. Majewski, "Imaging results of multimodal ultrasound computerized tomography system designed for breast diagnosis," *Computerized Medical Imaging and Graphics*, vol. 46, pp. 83–94, 2015.

[4] H. Gemmeke, L. Berger, T. Hopp, M. Zapf, W. Tan, R. Blanco, R. Leys, I. Peric, and N. V. Ruiter, "The new generation of the KIT 3D USCT," in *International Workshop on Medical Ultrasound Tomography*, vol. 1, pp. 271–281, KIT Scientific Publishing, 2018.

[5] N. V. Ruiter, M. Zapf, R. Dapp, T. Hopp, W. A. Kaiser, and H. Gemmeke, "First results of a clinical study with 3D ultrasound computer tomography," in *IEEE International Ultrasonics Symposium (IUS)*, pp. 651–654, 2013.

[6] M. Zapf, K. Hohlfeld, N. V. Ruiter, P. Pfistner, K. W. A. van Dongen, H. Gemmeke, A. Michaelis, and S. E. Gebhardt, "Development of single-fiber piezocomposite transducers for 3D ultrasound computer tomography," *Adv. Eng. Mater.*, vol. 20, p. 1800423, 2018.

[7] M. Angerer, M. Zapf, B. Leyrer, and N. V. Ruiter, "Semi-automated packaging of transducer arrays for 3D ultrasound computer tomography," in *IEEE Sensors*, pp. 1–4, IEEE, 2020.

[8] M. K. Feldman, S. Katyal, and M. S. Blackwood, "US artifacts," *RadioGraphics*, vol. 29, no. 4, pp. 1179–1189, 2009.

[9] R. De Luca, M. Bassani, L. Francalanci, F. Bertocci, F. Gelli, P. Palchetti, D. Coppini, and L. Bocchi in *A Mathematical Model for Reverberations in Biomedical Ultrasound Transducers: a case study*, IEEE, 2018.

[10] M. Angerer, M. Zapf, S. Gebhardt, H. Neubert, and N. V. Ruiter, "Enhanced KLM model for single-fibre piezocomposite transducers," in *IEEE Ultrasonics*, IEEE, 2020.

[11] E. L. Kinsler, *Fundamentals of Acoustics*. John Wiley and Sons, 4th ed., 2000.

[12] J. Koppenhöfer, *Measurement Environment for Acoustic Material Properties for Ultrasound Computed Tomography*. Thesis, Karlsruhe Institute of Technology, 2020.

[13] T. Szabo and J. r. Wu, "A model for longitudinal and shear wave propagation in viscoelastic media," *The Journal of the Acoustical Society of America*, vol. 107, pp. 2437–46, 2000.

[14] J. F. Guess and J. S. Campbell, "Acoustic properties of some biocompatible polymers at body temperature," *Ultrasound in Medicine and Biology*, vol. 21, no. 2, pp. 273–277, 1995.

[15] A. D. Nashif, D. I. Jones, and J. P. Henderson, *Vibration Damping*. John Wiley and Sons, 1986.

[16] X. Liu and Q. Feng, *Chapter 12 - Statistical energy analysis of tire/road noise*, pp. 271–296. Butterworth-Heinemann, 2020.

[17] L. Sperling and C. D. R., "Sound and vibration damping with polymers," *ACS Symposium Series*, vol. 424, pp. 5–22, 1990.